ACS APPLIED MATERIALS & INTERFACES

Research Article

www.acsami.org

Antimicrobial Activity of Starch Hydrogel Incorporated with Copper Nanoparticles

María Emilia Villanueva,[*,†,‡] Ana María del Rosario Diez,[†] Joaquín Antonio González,[†,‡] Claudio Javier Pérez,[§] Manuel Orrego,[∥] Lidia Piehl,[∥] Sergio Teves,[⊥,▽] and Guillermo Javier Copello[*,†,‡]

[†]Cátedra de Química Analítica Instrumental, Facultad de Farmacia y Bioquímica, Universidad de Buenos Aires, Junín 956, C1113AAD Buenos Aires, Argentina

[‡]Instituto de Química y Metabolismo del Fármaco, Facultad de Farmacia y Bioquímica, Universidad de Buenos Aires and Consejo Nacional de Investigaciones Científicas y Técnicas, Junín 956, C1113AAD Buenos Aires, Argentina

[§]Instituto en Investigaciones en Ciencia y Tecnologías de Materiales, Universidad de Mar del Plata and Consejo Nacional de Investigaciones Científicas y Técnicas, Juan B. Justo 4302, CP7600 Mar del Plata, Argentina

[∥]Cátedra de Física, Facultad de Farmacia y Bioquímica, Universidad de Buenos Aires, Junín 956, C1113AAD Buenos Aires, Argentina

[⊥]Cátedra de Microbiología, Facultad de Farmacia y Bioquímica, Universidad de Buenos Aires, Junín 956, C1113AAD Buenos Aires, Argentina

[▽]Proanalisis SA, Ángel Carranza 1941/7, C1414COW Buenos Aires, Argentina

Supporting Information

ABSTRACT: In order to obtain an antimicrobial gel, a starch-based hydrogel reinforced with silica-coated copper nanoparticles (Cu NPs) was developed. Cu NPs were synthesized by use of a copper salt and hydrazine as a reducing agent. In order to enhance Cu NP stability over time, they were synthesized in a starch medium followed by a silica coating. The starch hydrogel was prepared by use of urea and water as plasticizers and it was treated with different concentrations of silica-coated copper nanoparticles (Si−Cu NPs). The obtained materials were characterized by Fourier transform infrared (FT-IR) spectroscopy, electron paramagnetic resonance (EPR) spectroscopy, scanning electron microscopy (SEM), and rheometry. FT-IR and EPR spectra were used for characterization of Cu NPs and Si−Cu NPs, confirming that a starch cap was formed around the Cu NP and demonstrating the stability of the copper nanoparticle after the silica coating step. SEM images showed Cu NP, Si−Cu NP, and hydrogel morphology. The particle size was polydisperse and the structure of the gels changed along with particle concentration. Increased NP content led to larger pores in starch structure. These results were in accordance with the rheological behavior, where reinforcement by the Si−Cu NP was seen. Antimicrobial activity was evaluated against Gram-negative (*Escherichia coli*) and Gram-positive (*Staphylococcus aureus*) bacterial species. The hydrogels were demonstrated to maintain antimicrobial activity for at least four cycles of use. A dermal acute toxicity test showed that the material could be scored as slightly irritant, proving its biocompatibility. With these advantages, it is believed that the designed Si−Cu NP loaded hydrogel may show high potential for applications in various clinical fields, such as wound dressings and fillers.

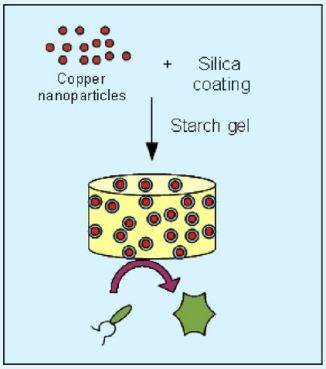

KEYWORDS: *starch hydrogel, copper nanoparticles, wound dressing, antimicrobial material, reinforcement*

INTRODUCTION

Copper and its complexes have been used since ancient times as disinfectants due to their antibacterial and antiviral properties.[1,2] In recent decades, with the development of nanoscience and nanotechnology, promising opportunities for examining the bactericidal effect of metal nanoparticles were presented.[3−5] The small size and high surface-to-volume ratio of copper nanoparticles (Cu NPs), in comparison with copper salts, allow them to interact closely with the membranes of microorganisms, enhancing their biocidal effect. Besides, their antimicrobial activity is not merely due to the release of metal ions in solution but also to the generation of reactive oxygen species (ROS) with subsequent oxidative damage to cellular structures.[5,6]

Although ionic copper is less toxic than ionic silver, the latter has been much more extensively studied for its use in the development of antimicrobial systems, either in its ionic form or in the nanoparticle form.[7−11] The main reason for this disparity relies on the instability of Cu NPs toward oxidation in air or aqueous media.[12,13] Thus, with the aim of using less toxic antimicrobials, Cu NPs have been studied by means of

Received: March 9, 2016
Accepted: June 13, 2016
Published: June 13, 2016

DOI: 10.1021/acsami.6b02955
ACS Appl. Mater. Interfaces 2016, 8, 16280−16288

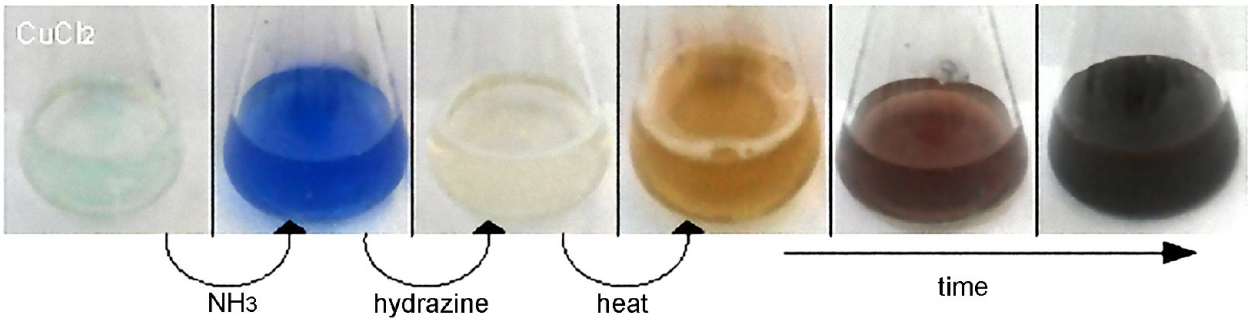

Figure 1. Pictures of different steps in Cu NP synthesis.

increasing their stability. An inert atmosphere is often used during synthesis. Another way to achieve Cu NP stabilization is use of a nonaqueous solvent[14−16] or a water-in-oil emulsion.[17] In the literature, many strategies to achieve Cu NP synthesis in water can be found: for instance, protection of nanoparticles during the reaction, either by adding surface-protecting agents, like organic ligands and inorganic capping materials, or by immersion in inert environments such as inorganic matrices and polymers.[18−21] Other approaches seek stabilization by using a silica coating of metallic nanoparticles.[22]

It is expected that, upon achievement of stable Cu NPs, their applicability as constituents of biomaterials will be promoted in the fields of medicine, biotechnology, etc. In this regard, hydrogels have wide applications in many fields such as agriculture, drug delivery, tissue engineering, water purification, contact lenses, sensors, wound dressings, etc.[23] Hydrogels are defined as hydrophilic, three-dimensional networks held together by chemical or physical bonds with corresponding water absorption capacity up to 10 g/g.[23,24] Starch hydrogels are becoming more and more important, and several examples of this kind of development are found in the literature, not only because of their low cost and abundance but also because of their biocompatibility and biodegradability.[23,25−28]

The aim of this paper was to combine a starch hydrogel with Cu NPs coated with silica to obtain a reinforced material with antimicrobial activity. Cu NPs were synthesized by use of a copper salt and hydrazine as a reducing agent. In order to enhance Cu NP stability, a starch medium was used during the reduction, followed by a silica coating method. The starch hydrogel was prepared by use of urea and water as plasticizers. The starch hydrogel was treated with different concentrations of silica-coated copper nanoparticles (Si−Cu NPs). The obtained materials were characterized by scanning electron microscopy (SEM), Fourier transform (FT-IR) and electron paramagnetic resonance (EPR) spectroscopy, and rheometry. Antimicrobial activity was evaluated against Gram-negative and Gram-positive bacterial species. Biocompatibility was evaluated by a dermal acute toxicity test.

EXPERIMENTAL SECTION

Materials. Copper(II) chloride and hydrazine were purchased from Biopack (Buenos Aires, Argentina). Corn starch was acquired from Unilever (Buenos Aires, Argentina). Sodium silicate was purchased from Sigma−Aldrich. *Staphylococcus aureus* ATCC 29213 was generously provided by the Microbial Culture Collection of Facultad de Farmacia y Bioquímica (CCM 29), University of Buenos Aires, and *Escherichia coli* wild type was isolated from a hospital environment. All microorganisms were grown at 35 °C for 24 h on Luria−Bertani (LB) medium (Britania, BA, Argentina).

Copper Nanoparticle Preparation. For Cu NP preparation, a metal salt precursor (copper chloride solution, 0.05 M) was used and the stabilizing agent was a 1% (w/v) aqueous starch solution. Equal volumes of starch and copper salt solutions were poured into a glass receptacle, and the pH was adjusted to 10 by use of concentrated ammonia solution. Hydrazine (5% w/v) was used as the reducing agent. Hydrazine solution (2 mL) was added to the starch/copper chloride solution and left in a 90 °C bath until the blue transparent solution, which had changed to pale yellow after reducing agent treatment, changed to the characteristic red color upon heating, indicating the formation of Cu NP (Figure 1). The nanoparticles were washed three times with 1% starch solution.

The reduction reaction can be expressed as

$$2Cu(NH_3)_2^{2+} + N_2H_4 + 4OH^- \rightarrow 2Cu + N_2 + 4NH_4OH \quad (1)$$

Copper Nanoparticle Silica Coating. In order to enhance Cu NP stability, a silica coating was performed via an inverse emulsion. Ethanol (60.0 mL) and Tween 20 (2.0 g) were stirred to obtain the organic phase. After that, a sodium silicate solution (2.3×10^{-2} g/mL) was prepared and mixed with 10.0 mL of an aqueous suspension of Cu NP (18.7 mM Cu). The aqueous phase was added dropwise to the organic phase and left with agitation for 18 h. After that time, it was centrifuged and washed three times with distilled water. This product was named Si−Cu NP.

Reaction Efficiency and Copper Content Determination. To assess Cu NP formation efficiency, the obtained suspension (1 mL) was centrifuged, the supernatant was discarded, and 1 mL of HNO_3 (0.6 N) was added to dissolve Cu NP and Si−Cu NP. The coated nanoparticles were sonicated at 35 kHz for 1 h in order to facilitate copper dissolution. After that, ammonia (0.2 mL) was added to form $Cu(NH_3)_2^{2+}$. The solution absorbance was measured at 618.5 nm and compared with a calibration curve. The yield of the synthetic Cu NP reaction and Cu concentrations in Cu NP and Si−Cu NP were calculated.[29]

Hydrogel Preparation and Copper Quantification. First, 10 g of urea, 100 g of starch, and different dilutions of a Si−Cu NP suspension (40.1 mM Cu) were mixed and hydrated with 400 mL of water. In order to plasticize the starch, the mixture was heated at 90 °C for 0.5 h with constant stirring. To obtain the hydrogels, the mixture was placed between two glasses and allowed to reach ambient temperature. Afterward, the gels were stored at −20 °C for 18 h. A gel without copper nanoparticles was also prepared as a control sample. The gels were cut into discs of 0.8 cm diameter. The hydrogel thickness was 0.3 cm.

Copper quantification in the gels before and after the antimicrobial assays was performed as follows: First the gels were digested in acidic medium in a HNO_3/H_2O_2 (10:1) solution for 10 min. Then the Cu content was quantified by capillary electrophoresis (Agilent Technologies; capillary column 75 μm × 30 cm, background electrolyte imidazole (6 mM) and hydroxyisobutyric acid (HIBA, 10 mM) pH 4.0, voltage +30 kV, injection 5 s, 10 mbar).

Spectroscopic and Microscopic Characterization. Cu NPs, Si−Cu NPs, and starch were placed in a quartz tube, and electron paramagnetic resonance (EPR) spectra were recorded at 20 °C in an

DOI: 10.1021/acsami.6b02955
ACS Appl. Mater. Interfaces 2016, 8, 16280−16288

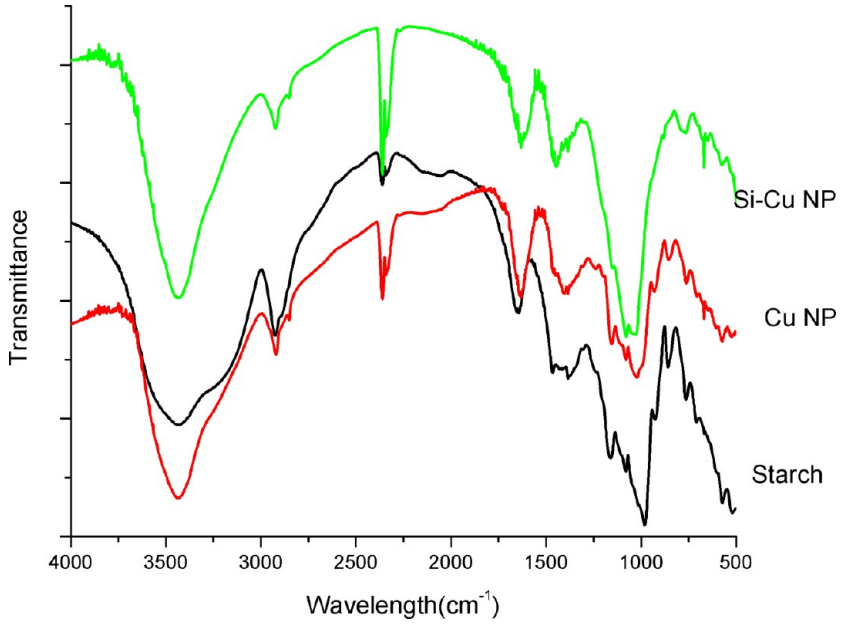

Figure 2. FT-IR spectra of starch, Cu NP, and Si−Cu NP.

X-band ESR spectrometer, Bruker EMX plus (Bruker Instruments, Inc., Berlin, Germany). The spectrometer settings were sweep width 1200.0 G and center field 3300 G. Microwave power for all measurements was 10.0 mW, and modulation amplitude was 0.5 G (conversion time 5.12 ms). Diphenylpicrylhydrazyl (DPPH, Aldrich) was used as an internal reference for g factor calculation, with g = 2.0036. Infrared spectra were acquired in the transmission mode, range 4000−650 cm^{-1}, on a Nicolet 360 FT-IR spectrometer. Water-band contribution was minimized by drying all samples at 60 °C for 24 h before the measurements. Electron microscopic images were obtained on a Zeiss Supra 40 scanning electron microscope. The Cu NPs and Si−Cu NPs were previously dried at 60 °C and the gels were freeze-dried. All the samples were coated with platinum.

Rheological Behavior. The linear viscoelastic range (LVR) of the samples was determined by amplitude sweeps. Then the elastic or storage modulus $G'(\omega)$, the viscous or loss modulus $G''(\omega)$, and complex viscosity η^* were determined at room temperature (20 °C) by a small-amplitude oscillatory shear flow assay with an Anton Paar (MCR-301) rotational rheometer equipped with a CTD 600 thermo chamber. Parallel plates (25 mm diameter) and a frequency range of 0.1−500 s^{-1} were used in all measurements. The gap width used was 1−3 mm. Small strains (γ = 0.2%) were used to ensure the linearity of the dynamic responses. A new sample was used for each replicate.[30]

Water Uptake. Hydrogel samples (preweighed and completely dried) were placed in 5.0 mL of distilled water for 30 min at 20 °C. After that time, the swollen gels were taken out, dried superficially with a filter paper to remove the water in the surface, and then weighed.[31] Percent water uptake was determined by

$$\%\text{water uptake} = \frac{M_f - M_0}{M_0} \times 100 \quad (2)$$

where M_f and M_0 are the final and initial mass, respectively.

Antimicrobial Activity Assay. Antimicrobial activity assay of the coatings against *E. coli* and *S. aureus* was carried out according to a modified assay from Japanese Industrial Standards (JIS) Z 2801, using microorganisms grown in LB medium for 24 h.[32] Preparation of the inoculum was achieved by diluting LB broth with sterile physiological solution to a 500-fold volume. Then, the inoculum was prepared by diluting the original inoculum until the microorganism concentration was 2.4 × 10^5 colony-forming units (cfu)/mL for *E. coli* and 1.7 × 10^5 cfu/mL for *S. aureus*. Each sample was inoculated with 0.010 mL of the previously described bacterial suspensions.

After 24 h of interaction between the samples and the bacterial suspension at 35 °C, the surviving bacteria were enumerated by the spread plate method. Ten-fold dilutions were spread on a Petri dish containing LB agar and incubated at 35 °C overnight. After incubation, the colonies were counted.[33] The results were presented in terms of value of antimicrobial activity [R(log), eq 3] and percent bacterial reduction (D, eq 4):

$$R(\log) = \log A - \log B \quad (3)$$

$$D = \frac{A - B}{B} \times 100 \quad (4)$$

where A is the average number of viable bacterial cells in the 0.00 mmol of Cu/g of starch hydrogel samples after 24 h and B is the average number of viable bacterial cells in the different treated samples after 24 h.

Acute Skin Irritation Test. Acute skin irritation of three starch hydrogels (0.00, 0.82, and 1.27 mmol of Cu/g of gel) was evaluated on rabbits by the OECD/OCDE 404 test.[34] This test was performed in a laboratory accredited by OECD[35] following a procedure in compliance with Good Laboratory Practice (GLP) standard 7.35. New Zealand albino rabbits weighing 2.1−3.5 kg were used. The animals were provided with food and water ad libitum in a temperature-controlled room (21 ± 5 °C) and exposed to light−dark cycles of 12 h. Twenty-four hours prior to beginning the study, an area on the back of rabbits was shaved (8 × 8 cm) and then washed with purified water. Each rabbit was treated with 0.00, 0.82, and 1.27 mmol of Cu/g of gel starch hydrogels, applied over a 1 cm^2 area of hair-free skin for 4 h. The skin was observed for erythema (reddening) or edema (swelling) at 24, 48, and 72 h after application and assigned values between 0 and 4 according to the test score.

Statistics. Triplicate samples of all quantitative results were carried out. Data were expressed as means ± standard deviation (SD). Statistical analysis was performed by a one-way analysis of variance (ANOVA) test and a Tukey post-test. A value of $p < 0.05$ was considered to be statistically significant.

RESULTS AND DISCUSSION

Copper Nanoparticle Synthesis Efficiency and Copper Content Determination. The yield of Cu NP synthesis was 74.8%. With this result we can conclude that the Cu NP formation reaction efficiency was high and a minimal amount of product was lost during washing steps. Stability in aqueous

DOI: 10.1021/acsami.6b02955
ACS Appl. Mater. Interfaces 2016, 8, 16280−16288

medium of these nanoparticles was greater than for those not synthesized in a starch medium. However, the stability could be improved. Hydrogels prepared with Cu NPs showed random stability and a fast and heterogeneous reversion to Cu^{2+} was observed. This oxidation was also observed in antimicrobial assays, which showed nonreproducible results.

In order to achieve the greatest possible stability over time, a silica coating was performed. Si−Cu NPs showed greater stability over time and in different storage conditions (solid and liquid media). The gels prepared with Cu NPs without the silica coating were not as stable as those prepared with Si−Cu NPs. This was evident by observing the characteristic blue color of Cu^{2+} within 24 h of storage. Therefore, the Cu NP-containing gels were discarded and the subsequent assays were performed with Si−Cu NP gels.

Once particle synthesis was optimized, three different dilutions of Si−Cu NP were performed and included in a starch gel. The Cu contents of those gels were 0.36, 0.82, and 1.27 mmol/g of gel.

Fourier Transform Infrared Spectroscopy. In Figure 2 the FT-IR spectra of Cu NP, Si−Cu NP, and starch are shown. In the starch spectrum the following bands were present: a broad and strong band between 3726 and 3007 cm^{-1}, corresponding to stretching of -OH groups; bands between 2920 and 2950 cm^{-1}, corresponding to -CH and -CH_2; bands at 1168, 1082, and 984 cm^{-1}, corresponding to vibrations of the -C−O−C- bonds in glucose; and bands at 931, 861, 771, 714, 608, and 575 cm^{-1}, ascribed to the pyranose ring. When the spectra of Cu NP and starch were compared, no significant differences could be observed, and it was concluded that the nanoparticles were surrounded by a starch layer that would provide them oxidation stability. The Si−Cu NP spectrum presented the same bands as the other two, except for the inverted intensities in bands at 1082 and 1032 cm^{-1}, which may be due to a contribution of Si−O−Si stretching of the silica coating. Also in this spectrum, the signals at 931 and 861 cm^{-1} disappeared and the signal found at 771 cm^{-1} was wider. The latter band corresponded to the symmetric vibration of Si−O group.

In Figure S1, FT-IR spectra of Si−Cu NP-containing starch hydrogels are shown. Due to the low amount of NP introduced in the gels, no signals aside from those of the starch could be observed.

Electron Paramagnetic Resonance. Copper state during the synthesis of NP was followed by EPR, making use of the paramagnetic properties of Cu(II) (d^9, $S = {}^1/_2$, $I = {}^3/_2$). Figure 3 shows EPR spectra for $CuCl_2$ used in the synthesis and for Cu NP and Si−Cu NP powders, together with simulations. Table 1 shows the values of **g** and **A** tensors calculated by simulation. $CuCl_2$ spectrum showed axial symmetry, with $g_x = g_y \gg g_z$ ($g_\perp$ and $g_\parallel$, respectively), in which four of the ligands were in a plane and close to copper atom, thus tightly bound, and the other two ligands were bound to an axis perpendicular to the former, generally with weak bonds.[36] After the reduction, no Cu(II) signal was observed (Figure 3b). As elementary copper is not paramagnetic, the absence of a detectable signal demonstrated an efficient reduction of the metal. After the silica coating step, a weak Cu(II) signal appeared in the spectrum where a change in the symmetry of the ligands could be observed. The axial symmetry was maintained but with a ratio $g_z > g_x = g_y$ ($g_\parallel$ and $g_\perp$, respectively) and a smaller difference between the **g** tensor values. Also, an intense hyperfine coupling (A_z) could be observed. The literature

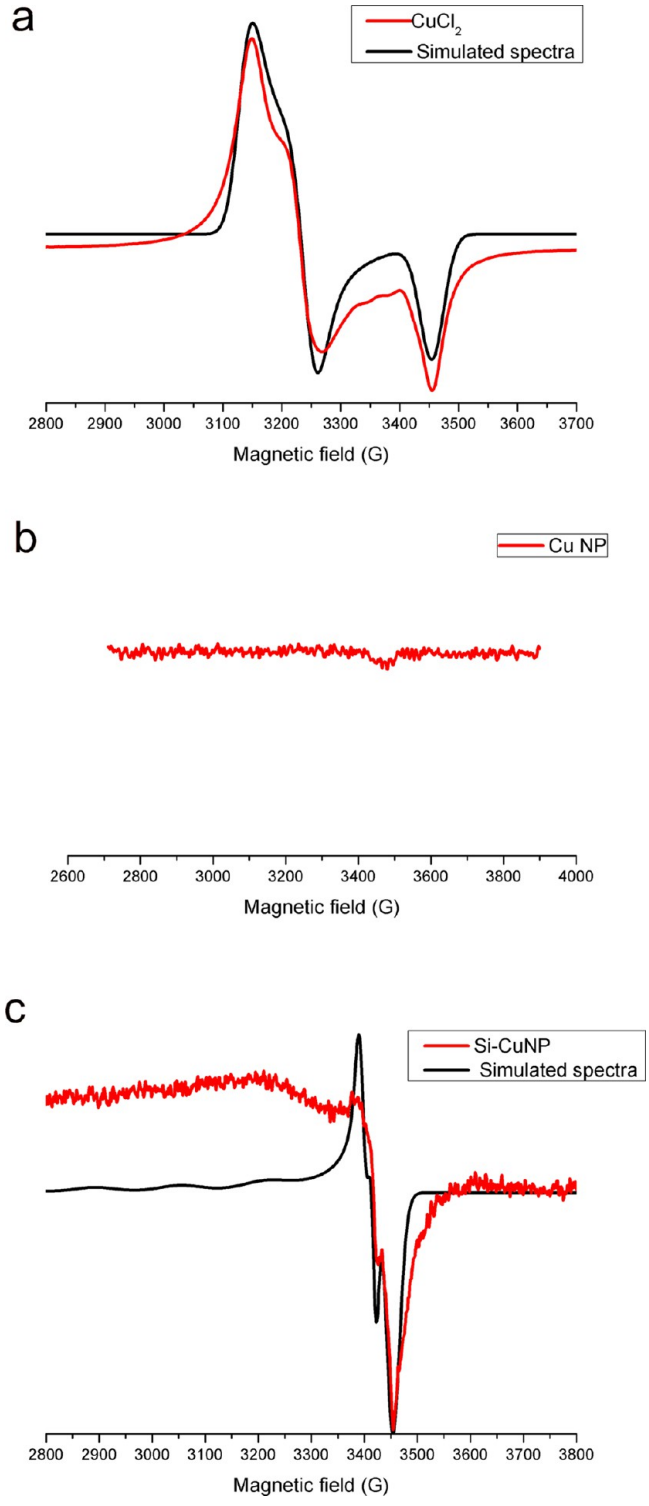

Figure 3. EPR spectra of (a) $CuCl_2$, (b) Cu NP powder, and (c) Si−Cu NP powder.

Table 1. g and A Tensors Calculated by Simulation

sample	g_x	g_y	g_z	A_x (G)	A_y (G)	A_z (G)
$CuCl_2$	2.2144	2.2144	2.0467	27	5	ND[a]
Cu NP	ND	ND	ND	ND	ND	ND
Si−Cu NP	2.0704	2.0704	2.3902	10	10	160

[a]Not detected.

DOI: 10.1021/acsami.6b02955
ACS Appl. Mater. Interfaces 2016, 8, 16280−16288

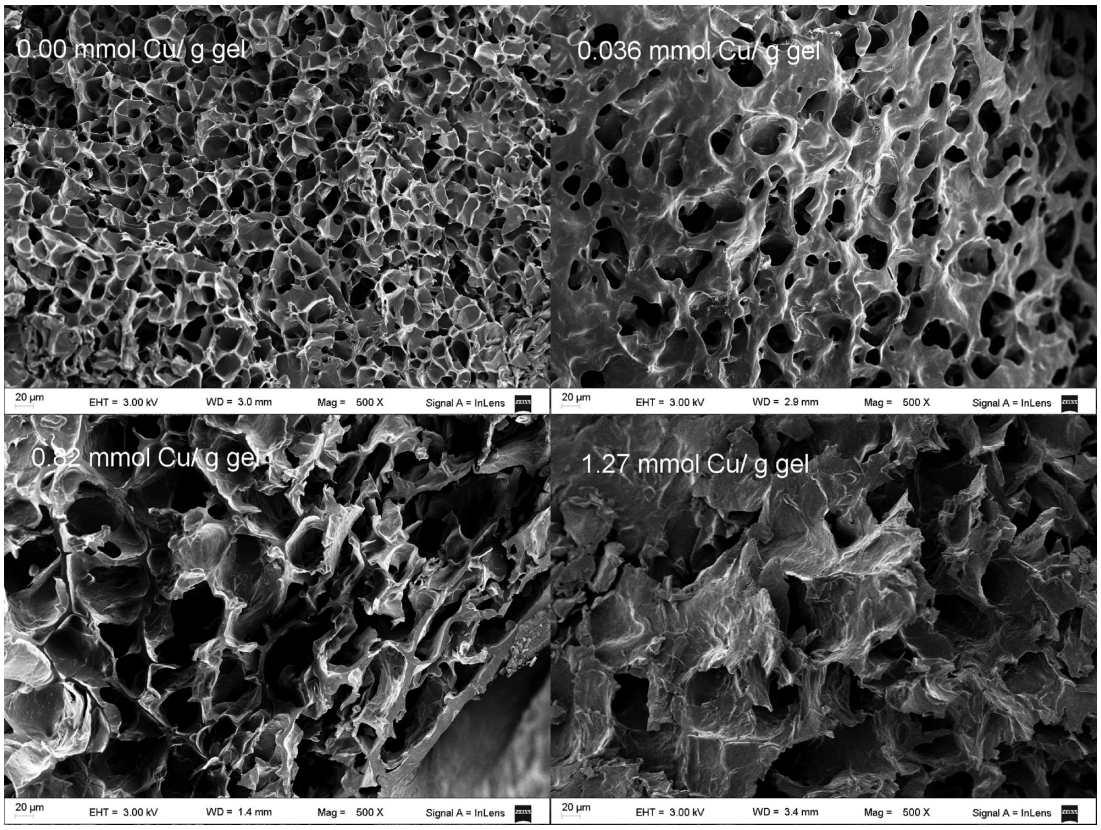

Figure 4. SEM images of starch hydrogel with different Si−Cu NP proportions (500×).

assigned such signals to strong adsorption of copper ions on a surface or to its immobilization on a material framework.[37] Thus, during the silica coating stage, a fraction of the copper could be oxidized to Cu(II) and be tightly retained at the nanoparticle surface.

Scanning Electron Microscopic Images. Figure S2 shows the morphology of Cu NP and Si−Cu NP. The particle size was polydisperse and varied approximately between 63 and 160 nm in diameter. Si−Cu NP were spherical and their size was polydisperse. Their sizes varied between 125 and 938 nm. By analysis of these images, it can be concluded that the silica coating was successful.

Macroscopic analysis of gels showed a product with spongelike characteristics. This structure could have been due to the low temperatures to which the samples were subjected after formation of the hydrogel. This morphology might be due to retrogradation of amylose and amylopectin added to ice crystal growth and recrystallization.[38]

The microstructure of the starch gels is displayed in Figure 4. All images showed a thick fibrillar network structure similar to a sponge, confirming what was observed macroscopically. This figure also showed how the microstructure of the gel varied with the concentration of nanoparticles. The sample with 0.00 mmol Cu/g of gel presented a mesh with pores evenly dispersed. As the proportion of Si−Cu NP increased, the morphology changed. Although a cross-linked material could be observed, the pores were less numerous and larger, and more open structures were formed by the collapse of the starch structure.

In Figure 5 the same gels are shown with higher magnification. In these images, the presence of particles was observed in all samples. In addition, it could be observed that the morphology of Si−Cu NP at different concentrations remained the same. These images demonstrate the stability of the nanoparticles through the hydrogel synthesis procedure.

Rheological Behavior. Figure 6 demonstrates the rheological behavior of the hydrogels. Figure 6a shows that G' was higher than G'' in all cases, which meant that the elastic component of the material is dominant over the viscous behavior, a typical characteristic of the behavior of a gel-like material.[30] Also, G' increased with Si−Cu NP content (Figure 6b), demonstrating that the addition of Si−Cu NP reinforced the material. These results showed that addition of the particles not only provides antimicrobial properties to the material but also endows it with greater strength, facilitating its manipulation and application.

Figure 6c shows the complex viscosity of the gels according to the frequency. In all samples, the complex viscosity decreased linearly with the rise of frequency, which implied a shear thinning behavior in which the material becomes more fluid as the applied frequency increases. This would be related to the polymer structure of starch and its bonding.

Water Uptake. Water uptake was 108.8% ± 12.8% for the sample with 0.00 mmol of Cu/g of gel; 108.5% ± 6.4% for the sample with 0.36 mmol of Cu/g of gel; 87.4% ± 10.0% for the sample with 0.82 mmol of Cu/g of gel; and 70.9% ± 15.3% for the sample with 1.27 mmol of Cu/g of gel. These results showed that water uptake decreased with increasing particle concentration. Although the difference between the samples with 0.36 and 1.27 mmol of Cu/g of gel was significant ($p < 0.05$), water uptake fell only 30%.

Interaction of a polymer chain with the surface of a nanoparticle implies a local heterogeneity with respect to polymer segmental mobility. Due to the high surface-to-volume

DOI: 10.1021/acsami.6b02955
ACS Appl. Mater. Interfaces 2016, 8, 16280−16288

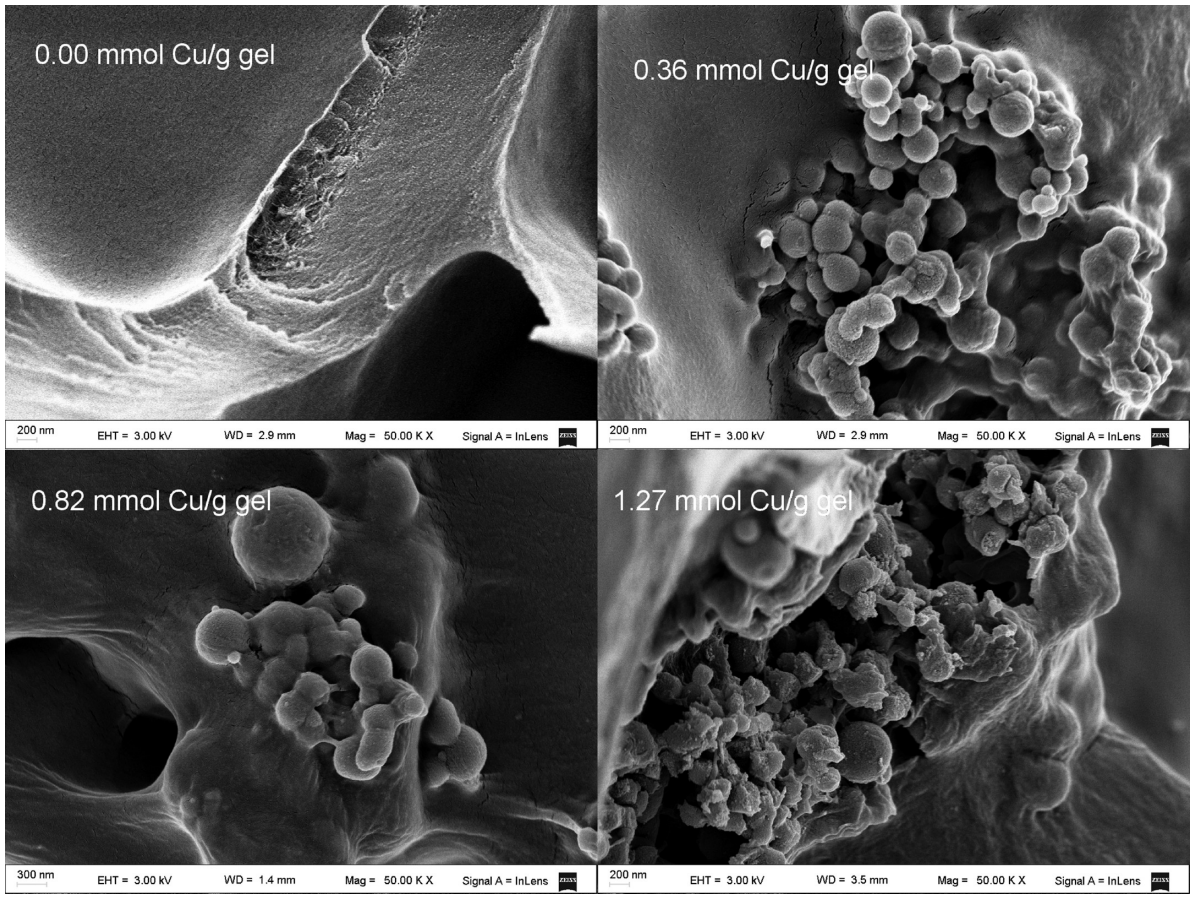

Figure 5. SEM images of starch hydrogel with different Si−Cu NP contents (50K×).

ratio of the nanoparticle, this effect can be remarkable with little nanoparticle content and will exert a response in the macroscopic properties of the material.[39] In particular, the behavior generally observed as reinforcement (increase in elastic modulus) can be atrributed to the interaction of polymer chains with the nanoobject, which leads to molecular stiffening and the consequent rearrangement of polymer structure.[40] As can be seen in Figure 4, the overall effect of the interaction of Si−Cu NPs would be a rearrangement of starch chains leading to wider and fewer pores as the amount of nanoparticles increases. This would be the main reason for the reinforcement produced by the nanoparticles, which was observed in the rheology assays. When it is taken into account that the mass of Si−Cu NPs is negligible in the bulk material and that water uptake diminishes with increasing NP content, probably the starch chains would be prone to interact with themselves rather than to be loosely extended in the bulk of the material and be available for interaction with water.

Antimicrobial Activity. Antimicrobial assay results (Table 2) indicate that the samples containing Si−Cu NP showed antimicrobial activity against both Gram-positive (*S. aureus*) and Gram-negative (*E. coli*) bacteria. The *R*(log) value was above 2 in all cases, which is the value required by the JIS standard to consider a material as an effective antimicrobial. The antimicrobial activity increased along with Si−Cu NP content.

As an additional test, elution of Cu was evaluated by determination of the presence or absence of an inhibition zone in subsequent incubations of the gels in inoculated agar plates. This assay was performed in agreement with Standard SNV 195920−1992.29.[41] The antibacterial property is defined as "good" when an inhibition zone is observed both close to and under the gel; it is defined as "sufficient" when growth inhibition area is observed under the sample only and as "not sufficient" if the sample is totally covered by bacteria as well as the area under the gel. The results of this test can be seen in Table 3 and Figure S3. An inhibition zone (defined as good) was observed for at least four passages in all treated samples, showing that the antibacterial effect was achieved due to biocidal release to the media. When the activity was evaluated against *S. aureus*, there was an inhibition zone in all the cases except the sample without Si−Cu NP and the sample with 0.36 mmol of Cu/g of gel in the fourth cycle. On the contrary, when the gels were evaluated against *E. coli*, antimicrobial activity was observed in all treated samples but not in the sample with 0.00 mmol of Cu/g of gel. These results, and those shown in Table 2, suggested that Si−Cu NP are more effective against Gram-negative than Gram-positive bacteria.

In order to determine copper elution, the content of copper in the composite hydrogel was determined before and after the antimicrobial activity assay. Results indicate that copper elution from the hydrogel is too little to accurately determine a difference between treatments.This also supports the stability conferred by silica capping.

Acute Dermal Irritation Test. Figure S4 shows a representative photograph of the back of rabbits after application of gels and controls. After 4 h of exposure, the samples with 1.27 mmol of Cu/g of gel presented a score of edema of 1 (very slight) and a score of erythema of 2 (well-defined erythema). The samples with 0.82 and 0.00 mmol of

DOI: 10.1021/acsami.6b02955
ACS Appl. Mater. Interfaces 2016, 8, 16280−16288

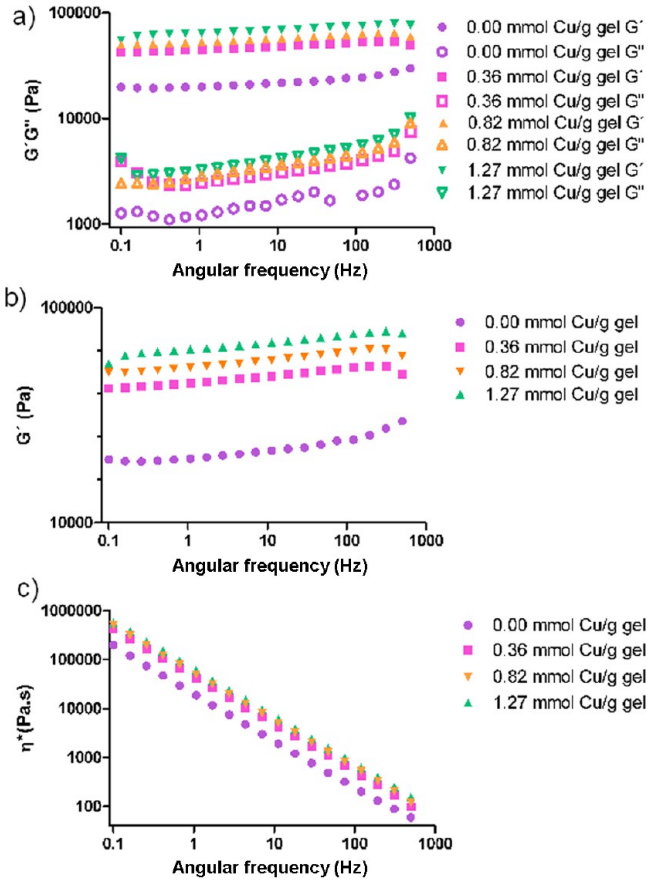

Figure 6. Frequency dependence of the storage modulus (G', solid symbols), loss modulus (G'', open symbols), and complex viscosity (η^*) of matrix starch gels with different contents of Si−Cu NP.

Table 2. Antimicrobial Activity against *S. aureus* and *E. coli*

Cu concn (mmol/g of gel)	cfu/mL	D (%)	R(log)
	S. aureus		
0	4.5×10^5		
0.36	4.0×10^3	98.665	2.6
0.83	100	99.977	3.6
1.27	1	99.999	5.7
	E. coli		
0	2.8×10^6		
0.36	300	99.900	4.2
0.83	33	99.992	3.7
1.27	1	99.999	5.7

Cu/g of gel presented no edema (score 0) and a score of 1 for erythema (very slight). Observational analysis of the skin surface of the rabbits over 24, 48, and 72 h post exposure showed a total absence of edema and erythema for all gels in all animals (score 0). According to the scoring, the gels could be classified as slightly irritating materials. These data denote the high biocompatibility of the new hydrogels.

CONCLUSION

In this research, a starch gel including silica-coated copper nanoparticles with antimicrobial activity was developed. Generally, the stability of Cu NPs is poor because they are easily oxidized in aqueous media and their stabilization is a challenging issue. We achieved their stabilization using two complementary techniques: first, starch capping during synthesis, and then, silica coating by inverse emulsion. The greatest stability over time obtained by the silica coating was probably achieved due to the physical barrier of the silica shell, which hindered interaction of oxygen molecules and Cu nanoparticles.[42]

Table 3. *S. aureus* and *E. coli* Growth Inhibition after Different Cycles

Cu concn (mmol of Cu/g of gel)	cycle number 1	2	3	4
	S. aureus			
0	not sufficient	not sufficient	not sufficient	not sufficient
0.36	good	good	good	not sufficient
0.82	good	good	good	good
1.27	good	good	good	good
	E. coli			
0	not sufficient	not sufficient	not sufficient	not sufficient
0.36	good	good	good	good
0.82	good	good	good	good
1.27	good	good	good	good

The yield of the nanoparticle synthesis was high (around 75%). SEM images showed that the Cu NP surface was rough. The particle size was polydisperse. In Si−Cu NP SEM images, their morphology was evaluated. Spherical and less rougher particles were obtained. These particles were also polydisperse. These Si−Cu NPs were immersed in starch gels. In the SEM images it could be observed that the structure of the gels changed along with particle concentration. The more concentrated gels showed larger pores. These results were in accordance with the rheological behavior, where reinforcement by Si−Cu NPs was observed.

In the antimicrobial efficacy studies, it was found that the gels are active against Gram-positive and Gram-negative bacteria. The mechanism of antimicrobial activity was demonstrated to be sustained release of the antimicrobial agent. A dermal acute toxicity test showed that the material could be scored as slightly irritant, proving its biocompatibility.

ASSOCIATED CONTENT

Supporting Information

The Supporting Information is available free of charge on the ACS Publications website at DOI: 10.1021/acsami.6b02955.

Four figures showing FT-IR spectra of different starch gels, SEM images of Cu NPs, photograph of agar diffusion test against *S. aureus*, and photographs of the back of rabbits after application of gels and controls (PDF)

AUTHOR INFORMATION

Corresponding Authors

*(M.E.V.) Telephone +54 11 49648254; fax +54 11 49648254; e-mail mevillanueva@ffyb.uba.ar.

*(G.J.C.) Telephone +54 11 49648254; fax +54 11 49648254; e-mail gcopello@ffyb.uba.ar.

Notes

The authors declare no competing financial interest.

DOI: 10.1021/acsami.6b02955
ACS Appl. Mater. Interfaces 2016, 8, 16280−16288

■ ACKNOWLEDGMENTS

M.E.V. is grateful for a postdoctoral fellowship granted by Consejo Nacional de Investigaciones Científicas y Técnicas (CONICET). J.A.G. is grateful for a doctoral fellowship granted by CONICET. This work was supported with grants from Universidad de Buenos Aires (UBACYT 20020130100780BA and 20020150200058BA), CONICET (PIP 11220120100657CO), and Agencia Nacional de Promoción Científica y Tecnológica [PICT-12-2663 (2014−2016) and 14-1919 (2016−2018)]. We thank Noah Dobin-Berstein for language corrections.

■ REFERENCES

(1) Li, P.; Xu, X.; Li, B.; Zhao, Y. Synthesis of Flower-like Sulfadiazine Copper/polyvinyl Pyrrolidone Composite and Its Antimicrobial Activities. *J. Nanopart. Res.* **2015**, *17* (9), 352.

(2) Dancer, S. J. Hospital Cleaning in the 21st Century. *Eur. J. Clin. Microbiol. Infect. Dis.* **2011**, *30* (12), 1473−1481.

(3) Hajipour, M. J.; Fromm, K. M.; Akbar Ashkarran, A.; Jimenez de Aberasturi, D.; Larramendi, I. R. de; Rojo, T.; Serpooshan, V.; Parak, W. J.; Mahmoudi, M. Antibacterial Properties of Nanoparticles. *Trends Biotechnol.* **2012**, *30* (10), 499−511.

(4) Liao, H.; Nehl, C. L.; Hafner, J. H. Biomedical Applications of Plasmon Resonant Metal Nanoparticles. *Nanomedicine* **2006**, *1* (2), 201−208.

(5) Ruparelia, J. P.; Chatterjee, A. K.; Duttagupta, S. P.; Mukherji, S. Strain Specificity in Antimicrobial Activity of Silver and Copper Nanoparticles. *Acta Biomater.* **2008**, *4* (3), 707−716.

(6) Lee, H.-J.; Song, J. Y.; Kim, B. S. Biological Synthesis of Copper Nanoparticles Using Magnolia Kobus Leaf Extract and Their Antibacterial Activity. *J. Chem. Technol. Biotechnol.* **2013**, *88* (11), 1971−1977.

(7) Flores, C. Y.; Miñán, A. G.; Grillo, C. A.; Salvarezza, R. C.; Vericat, C.; Schilardi, P. L. Citrate-Capped Silver Nanoparticles Showing Good Bactericidal Effect against Both Planktonic and Sessile Bacteria and a Low Cytotoxicity to Osteoblastic Cells. *ACS Appl. Mater. Interfaces* **2013**, *5* (8), 3149−3159.

(8) Song, J.; Kim, H.; Jang, Y.; Jang, J. Enhanced Antibacterial Activity of Silver/Polyrhodanine-Composite-Decorated Silica Nanoparticles. *ACS Appl. Mater. Interfaces* **2013**, *5* (22), 11563−11568.

(9) Rieger, K. A.; Cho, H. J.; Yeung, H. F.; Fan, W.; Schiffman, J. D. Antimicrobial Activity of Silver Ions Released from Zeolites Immobilized on Cellulose Nanofiber Mats. *ACS Appl. Mater. Interfaces* **2016**, *8* (5), 3032−3040.

(10) Zille, A.; Fernandes, M. M.; Francesko, A.; Tzanov, T.; Fernandes, M.; Oliveira, F. R.; Almeida, L.; Amorim, T.; Carneiro, N.; Esteves, M. F.; Souto, A. P. Size and Aging Effects on Antimicrobial Efficiency of Silver Nanoparticles Coated on Polyamide Fabrics Activated by Atmospheric DBD Plasma. *ACS Appl. Mater. Interfaces* **2015**, *7* (25), 13731−13744.

(11) Espinosa-Cristóbal, L. F.; Martínez-Castañón, G. A.; Martínez-Martínez, R. E.; Loyola-Rodríguez, J. P.; Patiño-Marín, N.; Reyes-Macías, J. F.; Ruiz, F. Antimicrobial Sensibility of Streptococcus Mutans Serotypes to Silver Nanoparticles. *Mater. Sci. Eng., C* **2012**, *32* (4), 896−901.

(12) Abdulla-Al-Mamun, M.; Kusumoto, Y.; Muruganandham, M. Simple New Synthesis of Copper Nanoparticles in Water/acetonitrile Mixed Solvent and Their Characterization. *Mater. Lett.* **2009**, *63* (23), 2007−2009.

(13) Khanna, P. K.; Gaikwad, S.; Adhyapak, P. V.; Singh, N.; Marimuthu, R. Synthesis and Characterization of Copper Nanoparticles. *Mater. Lett.* **2007**, *61* (25), 4711−4714.

(14) Park, B. K.; Jeong, S.; Kim, D.; Moon, J.; Lim, S.; Kim, J. S. Synthesis and Size Control of Monodisperse Copper Nanoparticles by Polyol Method. *J. Colloid Interface Sci.* **2007**, *311* (2), 417−424.

(15) Anžlovar, A.; Orel, Z. C.; Žigon, M. Copper (I) Oxide and Metallic Copper Particles Formed in 1, 2-Propane Diol. *J. Eur. Ceram. Soc.* **2007**, *27* (2), 987−991.

(16) Song, X.; Sun, S.; Zhang, W.; Yin, Z. A Method for the Synthesis of Spherical Copper Nanoparticles in the Organic Phase. *J. Colloid Interface Sci.* **2004**, *273* (2), 463−469.

(17) Qi, L.; Ma, J.; Shen, J. Synthesis of Copper Nanoparticles in Nonionic Water-in-Oil Microemulsions. *J. Colloid Interface Sci.* **1997**, *186* (2), 498−500.

(18) Huang, H. H.; Yan, F. Q.; Kek, Y. M.; Chew, C. H.; Xu, G. Q.; Ji, W.; Oh, P. S.; Tang, S. H. Synthesis, Characterization, and Nonlinear Optical Properties of Copper Nanoparticles. *Langmuir* **1997**, *13* (2), 172−175.

(19) Kobayashi, Y.; Shirochi, T.; Yasuda, Y.; Morita, T. Metal−metal Bonding Process Using Metallic Copper Nanoparticles Prepared in Aqueous Solution. *Int. J. Adhes. Adhes.* **2012**, *33*, 50−55.

(20) Valodkar, M.; Rathore, P. S.; Jadeja, R. N.; Thounaojam, M.; Devkar, R. V.; Thakore, S. Cytotoxicity Evaluation and Antimicrobial Studies of Starch Capped Water Soluble Copper Nanoparticles. *J. Hazard. Mater.* **2012**, *201−202* (0), 244−249.

(21) Mallick, S.; Sharma, S.; Banerjee, M.; Ghosh, S. S.; Chattopadhyay, A.; Paul, A. Iodine-Stabilized Cu Nanoparticle Chitosan Composite for Antibacterial Applications. *ACS Appl. Mater. Interfaces* **2012**, *4* (3), 1313−1323.

(22) Shiomi, S.; Kawamori, M.; Yagi, S.; Matsubara, E. One-Pot Synthesis of Silica-Coated Copper Nanoparticles with High Chemical and Thermal Stability. *J. Colloid Interface Sci.* **2015**, *460*, 47−54.

(23) Ismail, H.; Irani, M.; Ahmad, Z. Starch-Based Hydrogels: Present Status and Applications. *Int. J. Polym. Mater.* **2013**, *62* (7), 411−420.

(24) Kabiri, K.; Omidian, H.; Zohuriaan Mehr, M. J.; Doroudiani, S. Superabsorbent Hydrogel Composites and Nanocomposites: A Review. *Polym. Compos.* **2011**, *32* (2), 277−289.

(25) Pal, K.; Banthia, A. K.; Majumdar, D. K. Effect of Heat Treatment of Starch on the Properties of the Starch Hydrogels. *Mater. Lett.* **2008**, *62* (2), 215−218.

(26) Pal, K.; Banthia, A. K.; Majumdar, D. K. Preparation of Transparent Starch Based Hydrogel Membrane with Potential Application as Wound Dressing. *Trends Biomater Artif Organs* **2006**, *20* (1), 59−67.

(27) Zhai, M.; Yoshii, F.; Kume, T.; Hashim, K. Syntheses of PVA/starch Grafted Hydrogels by Irradiation. *Carbohydr. Polym.* **2002**, *50* (3), 295−303.

(28) Ramesh, M.; Mitchell, J. R.; Jumel, K.; Harding, S. E. Amylose Content of Rice Starch. *Starch/ Stärke* **1999**, *51* (8-9), 311−313.

(29) Mehlig, J. Colorimetric Determination of Copper with Ammonia. *Ind. Eng. Chem., Anal. Ed.* **1941**, *13* (8), 533−535.

(30) Ferry, J. D. *Viscoelastic Properties of Polymers*, 3rd ed.; John Wiley & Sons: 1980.

(31) Bajpai, S. K.; Singh, S. Analysis of Swelling Behavior of Poly(methacrylamide-Co-Methacrylic Acid) Hydrogels and Effect of Synthesis Conditions on Water Uptake. *React. Funct. Polym.* **2006**, *66* (4), 431−440.

(32) *JIS Z 2801: Antimicrobial Products—Test for Antimicrobial Activity and Efficacy*; Japan Standards Association, 2000.

(33) Gadenne, V.; Lebrun, L.; Jouenne, T.; Thebault, P. Antiadhesive Activity of Ulvan Polysaccharides Covalently Immobilized onto Titanium Surface. *Colloids Surf., B* **2013**, *112* (0), 229−236.

(34) Organization for Economic Cooperation and Development. Test No. 404: Acute Dermal Irritation/Corrosion. In *OECD Guidelines for Testing of Chemicals, Section 4: Health Effects*; OECD: 2015; DOI: 10.1787/20745788.

(35) *Certificado de Conformidad con los Principios de las Buenas Practicas de Laboratorio de la OCDE*; http://www.proanalisis.com.ar/img/acreditaciones/pdf/oecd.pdf. (Accessed 20 May 2016).

(36) Peisach, J.; Blumberg, W. E. Structural Implications Derived from the Analysis of Electron Paramagnetic Resonance Spectra of Natural and Artificial Copper Proteins. *Arch. Biochem. Biophys.* **1974**, *165* (2), 691−708.

DOI: 10.1021/acsami.6b02955
ACS Appl. Mater. Interfaces 2016, 8, 16280−16288

(37) Lin, F.; Meng, X.; Kukueva, E.; Altantzis, T.; Mertens, M.; Bals, S.; Cool, P.; Van Doorslaer, S. Direct-Synthesis Method towards Copper-Containing Periodic Mesoporous Organosilicas: Detailed Investigation of the Copper Distribution in the Material. *Dalton Trans.* **2015**, *44* (21), 9970−9979.
(38) Navarro, A. S.; Martino, M. N.; Zaritzky, N. E. Viscoelastic Properties of Frozen Starch-Triglycerides Systems. *J. Food Eng.* **1997**, *34* (4), 411−427.
(39) Arrighi, V.; McEwen, I. J.; Qian, H.; Prieto, M. B. S. The Glass Transition and Interfacial Layer in Styrene-Butadiene Rubber Containing Silica Nanofiller. *Polymer* **2003**, *44* (20), 6259−6266.
(40) Jancar, J.; Douglas, J. F.; Starr, F. W.; Kumar, S. K.; Cassagnau, P.; Lesser, A. J.; Sternstein, S. S.; Buehler, M. J. Current Issues in Research on Structure−property Relationships in Polymer Nanocomposites. *Polymer* **2010**, *51* (15), 3321−3343.
(41) *Textile Fabrics - Determination of the Antibacterial Activity - Agar Diffusion Plate Test*; Standard: SNV 195920; Schweizerische Normen-Vereinigung, 1992.
(42) Kobayashi, Y.; Sakuraba, T. Silica-Coating of Metallic Copper Nanoparticles in Aqueous Solution. *Colloids Surf., A* **2008**, *317* (1), 756−759.

DOI: 10.1021/acsami.6b02955
ACS Appl. Mater. Interfaces 2016, 8, 16280−16288